Journal of Orthopaedic Surgery and Research

RESEARCH

Open Access

Icariin promotes osteogenic differentiation of bone marrow mesenchymal stem cells (BMSCs) by activating PI3K-AKT-UTX/EZH2 signaling in steroid-induced femoral head osteonecrosis

Wei Ji[1†], Guoqing Gong[2†], Yuanhang Liu[1], Yan Liu[1], Jie Zhang[1] and Qiang Li[3*]

Abstract

Background Differentiation of bone marrow mesenchymal stem cells (BMSCs) is pivotal in the pathogenesis of steroid-induced femoral head osteonecrosis. Icariin, an active ingredient in Epimedii herba, has the potential to regulate osteogenic differentiation of BMSCs. Nevertheless, the related mechanism is still unclear. The study aimed to explore whether icariin can affect osteogenic differentiation by activating PI3K/AKT signaling to alter UTX and EZH2 expression and thus regulating osteogenesis-related genes in BMSCs.

Methods BMSCs were collected from Sprague Dawley rats and identified by measuring the positive ratios of cell markers using flow cytometry. Cells were treated with 1 μmol/L dexamethasone (DEX) for 24 h with or without 0.1–10 μM of icariin treatment. Cell counting Kit-8 (CCK-8) assays and flow cytometry analyses were performed to measure cell viability and apoptosis. Western blotting was conducted for measurement of apoptotic markers, factors involved in the PI3K/AKT-UTX/EZH2 pathway, osteogenic markers, and adipogenesis-related factors. Alizarin red S staining and Oil-red O staining were performed to measure the effect of DEX, icariin, UTX overexpression, or EZH2 knockdown on osteogenic and adipogenic differentiation of BMSCs.

Results Icariin ameliorated DEX-induced rat BMSC injury. Icariin activated the PI3K/AKT signaling, thereby upregulating UTX and phosphorylated EZH2 levels while inhibiting EZH2 and H3K27me3 expression. Additionally, icariin promoted osteogenic differentiation and inhibited adipogenic differentiation of BMSCs. Importantly, overexpressing UTX or silencing EZH2 exerted similar effects on BMSC differentiation as icariin did.

Conclusions Icariin promotes osteogenic differentiation of DEX-treated BMSCs by activating PI3K/AKT signaling to upregulate UTX and inhibit EZH2, finally inducing H3K27me3 depletion.

Keywords Adipogenesis, Icariin, BMSC, Osteonecrosis of femoral head, Osteogenic differentiation

†Wei Ji and Guoqing Gong contributed equally to this work.

*Correspondence:
Qiang Li
Liqiangmm@hotmail.com

Full list of author information is available at the end of the article

Introduction

Osteonecrosis of femoral head (ONFH) is a prevalent orthopedic disease characterized by osteocyte and bone marrow component necrosis, accompanied by alterations in the internal structure of the femoral head, ultimately resulting in collapse [1, 2]. In ONFH, the blood supply is inadequate to meet the metabolic demands of the bone [3]. Pathogenic factors for the disease include trauma, alcoholism, autoimmune diseases, hemoglobinopathy, and overuse of corticosteroids [4]. Magentic resonance imaging is regarded as a specific diagnostic tool for detection of early-stage ONFH [3]. Currently, the treatment options for ONFH include surgical management, conservative management, and total hip replacement [5]. A recent study has identified that following treatment for ONFH, adverse prognostic indicators include male patients, prolonged symptom duration prior to treatment, a high visual analog scale score, and reduced Harris Hip scores [6]. Steroid-induced ONFH (SONFH) accounts for most nontraumatic forms ONFH and is common in patients at young and middle age [7]. Although total hip arthroplasty can provide a cure, the current trend of younger patients with longer life expectancy than artificial joints implies that these individuals may undergo multiple revision surgeries [8]. At present, the precise mechanism underlying SONFH remains elusive; however, increasing evidence shows that there is a correlation between the disease and deficiencies in bone marrow mesenchymal stem cells (BMSCs) [8–10].

BMSCs are characterized with their capabilities of self-renewal, secretion of trophic factors, multiple differentiation, including differentiation into osteoblasts, adipocytes, chondrocytes, and endotheliocytes [11]. They play an important role in regulating bone metabolism and maintaining bone homeostasis [12]. Many studies have investigated the regeneration of tendon, bone, and cartilage using MSCs, owing to their multipotent differentiation potential and the relative ease of procurement [13]. The activities of BMSCs have garnered significant attention in studies focused on SONFH. For example, glucocorticoids promote ONFH by inducing oxidative stress and promoting BMSC apoptosis via the SIRT2/BMP2 axis [14]. Cyasterone, the natural ingredient in Achyranthes bidentata, is shown to protect rat BMSCs from dexamethasone (DEX)-induced apoptosis and thereby promote bone repair in the animal model of SONFH [15]. DEX is a common synthetic glucocorticoids with anti-inflammation and immunosuppression properties [16]. It has been verified to induce apoptosis of BMSCs and osteoblasts by activating caspases [17]. Caspase 3 together with other apoptotic proteins such as Bcl-2-associated X (Bax), B-cell lymphoma-2 (Bcl-2), and cleaved caspase-9 are key factors responsible for BMSC apoptosis [18]. Moreover, these apoptotic proteins are associated with PI3K/AKT pathway. Activation of the PI3K/AKT pathway can repress the apoptosis of BMSCs [19, 20].

The study aimed to explore the role of icariin, an active ingredient in the Chinese herbal medicine Epimedii herba, in DEX-stimulated BMSCs. A previous study showed that icariin mitigates iron overload-induced BMSC dysfunction by regulating mitochondrial fusion and fission via activation of the PI3K/AKT/mTOR and inhibition of the MAPK pathway [21]. In addition, icariin has been reported to protect BMSCs from glucocorticoid-induced injury and alleviate osteonecrosis in a rat model of glucocorticoid-related ONFH [22]. However, the underlying mechanism is still unclear. An article published in Science demonstrated that Akt inhibits methylation of H3K27 by mediating phosphorylation of enhancer of zeste homolog 2 (EZH2) [23]. Histone lysine demethylase 6a (known as UTX or KDM6A) is trimethylated histone 3 lysine 27 (H3K27me3) demethylase and has been discovered to be involved in the regulation of osteocyte differentiation [24]. Therefore, we hypothesized that icariin may alter UTX and EZH2 expression via the PI3K/AKT signaling, thereby regulating osteogenesis-related genes to affect osteogenic differentiation of BMSCs. The novelty of the present work refers to the relationship between icariin and the PI3K/AKT-UTX/EZH2 pathway in DEX-stimulated rat BMSCs. The study further investigated the mechanism underlying the protective role of icariin in ONFH.

Materials and methods

Isolation and culture of rat BMSCs

A total of 3 Sprague Dawley rats (4-week-old, 70 ± 0.5 g) were used for the harvest of rat BMSCs as previously described [25, 26]. All procedures were performed following the guidelines of the Declaration of Helsinki and were approved by Institutional Animal Care and Use Committee of Wuhan Myhalic Biotechnology Co., Ltd. After the rats were anesthetized and sacrificed via cervical dislocation, their bilateral femurs and tibias were then extracted with the removement of attached muscles. The bone marrow contents from femurs and tibias were collected using a 10 mL syringe. The contents were then carefully layered over an equal volume of Ficoll-Paque (Absin, Shanghai, China) and centrifuged at 900 g for 20 min at 4 °C. Subsequently, the intermediate phase containing the mononuclear cell layer was isolated and subjected to two rounds of washing.

The cells were cultured in osteogenic differentiation medium (HyCyte, Suzhou, China) added with 10% fetal bovine saline (FBS), 100 U/mL streptomycin, and 100 U/mL penicillin at 37℃ with 5% CO_2. After 48 h of cell culture, the adherent cells were cultured in another flask while the nonadherent cells were removed.

Identification of BMSCs

Flow cytometry was performed to identify BMSCs by measuring the positive ratios of CD44, CD29, CD45, and CD34. Cells were washed with phosphate buffered saline (PBS) and resuspended in PBS-2% bovine serum albumin at the concentration of 2×10^7 cells/ml. Primary antibodies (BD Biosciences) of CD44-fluorescein isothiocyanate (FITC), CD29-phycoerythrin (PE), CD45-PE, and CD34-FITC were incubated with the cell suspension at ambient temperature without light exposure. After incubation, the cells were washed with PBS twice, resuspended in 100 μL PBS, and analyzed using flow cytometry (Becton Dickinson, Franklin Lakes, USA).

Cell transfection

The plasmids of pORF-UTX were purchased from InvivoGene (Shanghai, China) and were used to amplify UTX expression. Short hairpin RNA targeting EZH2 (sh-EZH2) was synthesized from Genepharma (Shanghai, China) and was utilized to silence EZH2 expression. The pORF-UTX vectors (30 nM), the control vectors (30 nM), sh-EZH2 (40 nM), or sh-NC (40 nM) were transfected into BMSCs using Lipofectamine 3000 (Invitrogen, Carlsbad, USA) for 48 h.

Cell treatment

To establish the cell model of femoral head osteonecrosis, dexamethasone (DEX) was used to treat BMSCs at the concentration of 1 μmol/L for 24 h [26]. Icariin was purchased from MedChem Express (Monmouth Junction, USA) and dissolved in dimethyl sulfoxide with storage at -20℃ in the dark [22]. To explore its cytotoxicity, BMSCs were treated with 0.01, 0.1, 1, or 10 μM of icariin for 24 h. After that, 0.1, 1, or 10 μM of icariin was identified as low, medium, or high dose of icariin, respectively. DEX + parathyroid hormone (PTH) group was set as the positive control, and cells in this groups were treated with 10 nM PTH. The dose of PTH was identified according to a previous study [27]. To inhibit the PI3K/Akt signaling, BMSCs were treated with 10 μM LY294002 (Beyotime, Shanghai, China), an inhibitor for the PI3K pathway, for 30 min. The dosage of LY294002 was determined based on previously published studies [28, 29].

Cell viability detection

The viability of BMSCs was measured using Cell counting Kit-8 (CCK-8) assay kit (Solarbio, Beijing, China). Cells were inoculated into 96-well plates at the concentration of 5×10^3 cells/well and subjected to abovementioned treatment for 24 h. After that, complete medium (100 μL) containing 10 μL CCK-8 reagent were added to each well for 4 h of incubation. A microplate reader (Tecan, Switzerland) was used to assess the absorbance at 450 nm wavelength. Each assay was repeated in triplicate.

Flow cytometry analysis

BMSCs were seeded onto six-well plates until the confluence reaching ~ 80% and then subjected to DEX or icariin treatment. An AnnexinV-FITC/PI apoptosis detection kit (Vazyme, Nanjing, China) was used to stain BMSCs following the manufacturer's recommendations. A flow cytometry (Becton Dickinson) was utilized to quantify the proportion of apoptotic cells. The assay was repeated in thrice.

Alizarin red S staining

BMSCs were placed onto 6-well plates (3×10^5 cells/well). After 21 days of osteogenic induction culture, cells were fixed with 4% paraformaldehyde (Sigma Aldrich, St. Louis, USA) for 30 min and stained with alizarin red S staining solution (pH = 4.2, YaJi Biological, Shanghai, China) for 20 min at ambient temperature with gentle shaking. Then, cells were washed with distilled water three times. A fluorescence microscope (Olympus, Tokyo, Japan) was used to capture images.

RT-qPCR

Extraction of total RNA from BMSCs was performed utilizing TRIzol reagent (Invitrogen, Carlsbad, USA). RNA was reverse transcribed into cDNA using a first strand cDNA synthesis kit (TaKaRa, Japan). Quantitative PCR was performed using a SYBR premix qPCR kit (TaKaRa). The reaction was conducted under the following conditions: initial denaturation at 95 °C for 180 s, followed by 40 cycles of 95 °C for 15 s and annealing at 60 °C for 30 s. Relative gene expression was calculated using the 2ΔΔCt method with β-actin as the internal control. Primer sequences were listed in supplementary Table 2.

Induction of adipogenic differentiation and Oil-red O staining

BMSCs at passage 3 were seeded onto 24-well plate (5×10^5 cells/well) for culture. When cells reached 95–100% confluence, the culture medium was replaced with adipogenic differentiation medium (DMEM, 10% FBS, 0.2 mM indomethacin, 1 μM dexamethasone, 0.5 mM 3-isobutyl-1-methylxanthine, 10 μg/ml insulin). After 2 weeks of cell culture, cells were stained with oil red O solution (Solarbio, Beijing, China) in line with the protocol's instructions. A microscope (Nikon, Japan) was used to observe the formation of lipid droplets.

Animal model of SONFH

A total of 24 Sprague Dawley rats (250 ± 20 g, 7–8 weeks) were obtained from Vital River animal technology (Beijing, China). The rats were randomly assigned into three groups: control group, SONFH group, and SONFH + icarrin group ($n = 8$/group). This study received approval from the Animal Ethics Committee of Wuhan

Myhalic Biotechnology Co., Ltd (approval number: HLK-202309296; approval date: September 21, 2023). All experimental procedures were conducted in accordance with the ARRIVE guidelines.

A rat model of SONFH was established as previously described [30, 31]. In the SONFH group, rats were administered with lipopolysaccharide (LPS) at a dose of 10 μg/kg (Sigma-Aldrich, USA) via tail vein injection every 24 h for two consecutive days. This was followed by intramuscular injections of methylprednisolone (MPS) at 40 mg/kg into the gluteal muscle (alternating sides) at 24-h intervals for a total of three doses over one week. Additionally, to prevent infections, 80,000 units of sodium penicillin were injected intraperitoneally twice weekly. Rats in the control group were injected with the same amount of saline. In the SONFH + icarrin group, icarrin (purity: 99.06%, MedChem Express, USA) was given via gavage at a daily dose of 20 mg/kg after the first injection of MPS for six weeks. The dose of icarrin was identified according to previous studies [30, 32]. During the period of drug administration, animals in the control group and SONFH group received distilled water at the same volume.

Micro-computed tomography (micro-CT) analysis

The micro-CT was performed after modeling. The femur was harvested, and all surrounding muscles and soft tissues were carefully removed. The femoral samples were then fixed in a 4% paraformaldehyde solution before being scanned using micro-CT technology. Key trabecular parameters assessed included bone volume (BV, measured in cubic millimeters), bone volume fraction (BV/TV), trabecular number (Tb.N, per millimeter), and trabecular separation (Tb.Sp, in millimeters).

Hematoxylin-eosin (H&E) staining

The femurs were fixed in 4% paraformaldehyde (Sigma Aldrich, USA) and subsequently decalcified using a 10% ethylenediaminetetraacetic acid solution (Servicebio, Wuhan, China) for a period of four weeks. Following decalcification, the samples were embedded in paraffin. Longitudinal sections of the tissue were prepared, cut into 5 μm sections, and stained with hematoxylin-eosin (H&E; Solarbio, Beijing, China). The sections were then mounted with neutral gum and examined under a light microscope.

Western blotting

Total protein was isolated from cultured cells or rat femur tissues using lysis buffer containing phenylmethylsulfonyl fluoride (Zeye Biotechnology, Shanghai, China) on ice. The total protein concentration was determined using bicinchoninic acid assay kit (Biorbyt, UK). Next, the total protein (60 μg) was electrophoresed using 10–12% polyacrylamide gels and then transferred to PVDF membranes (Millipore, Billerica, USA). The membranes were blocked with 5% fat-free milk for 2 h at ambient temperature, followed by incubation with primary antibodies (supplementary Table 1) at 4℃ overnight. After that, the membranes were incubated with secondary antibodies for 1 h. β-actin was set as the loading control. The bands were illuminated using an enhanced chemiluminescence substrate kit (Thermo Fisher Scientific, Waltham, USA) and imaged using a Bio-Rad scanner. The density of blots was analyzed using ImageJ software.

Statistical analysis

Data are shown as the mean ± standard deviations. One-way analysis of variance was utilized to assess the differences among multiple groups using GraphPad Prism software (La Jolla, USA). The value of p less than 0.05 was set as the threshold for statistical significance.

Results

Morphology and identification of rat BMSCs

BMSCs were isolated from rats and cultured for indicated days. As shown by microscopy images in Fig. 1A, cells were in a spindle shape after 10 days of culture. Flow cytometry analysis was performed to detect the purity of BMSCs. Figure 1B showed that the percentages of CD29-PE- and CD44-FITC-positive BMSCs are 99.4% and 99.7%, while those of CD34- and CD45-positive BMSCs were 2.52% and 1.39%. The results showed that the cultured BMSCs positively expressed CD29 and CD44 while negatively expressed CD34 and CD45. The above data can identify that the cultured cells were BMSCs.

Icariin attenuates DEX-induced rat BMSC apoptosis

Before exploring the effect of icariin (Fig. 2A) on DEX-induced BMSC injury, the toxicity of icariin to BMSCs was first identified. Figure 2B displayed that the concentrations of 0.01 to 10 μM icariin exerted no significant damage to BMSCs. For subsequent experiments, three doses of 0.1 μM, 1 μM, and 10 μM were used and named as low, medium, and high doses of icariin, respectively. According to results of CCK-8 assays, DEX markedly lowered the viability of rat BMSCs (54.15%), and the trend was noticeably rescued by icariin treatment (Fig. 2C). Of note, the medium concentration of icariin most significantly increased cell viability to 85.4%, which was higher than both the low and high doses (68.11% and 73.56%). The value in the medium group is comparable to that observed in the DEX + PTH positive control group (87.4%) (Fig. 2C). In contrast, the apoptosis of BMSCs was enhanced by DEX treatment (18.36 ± 1.52%) compared with that in control group (5.26 ± 0.45%), while icariin prominently reduced the cell apoptotic rate in the context of DEX (10.15 ± 0.95%, 5.82 ± 0.53%,

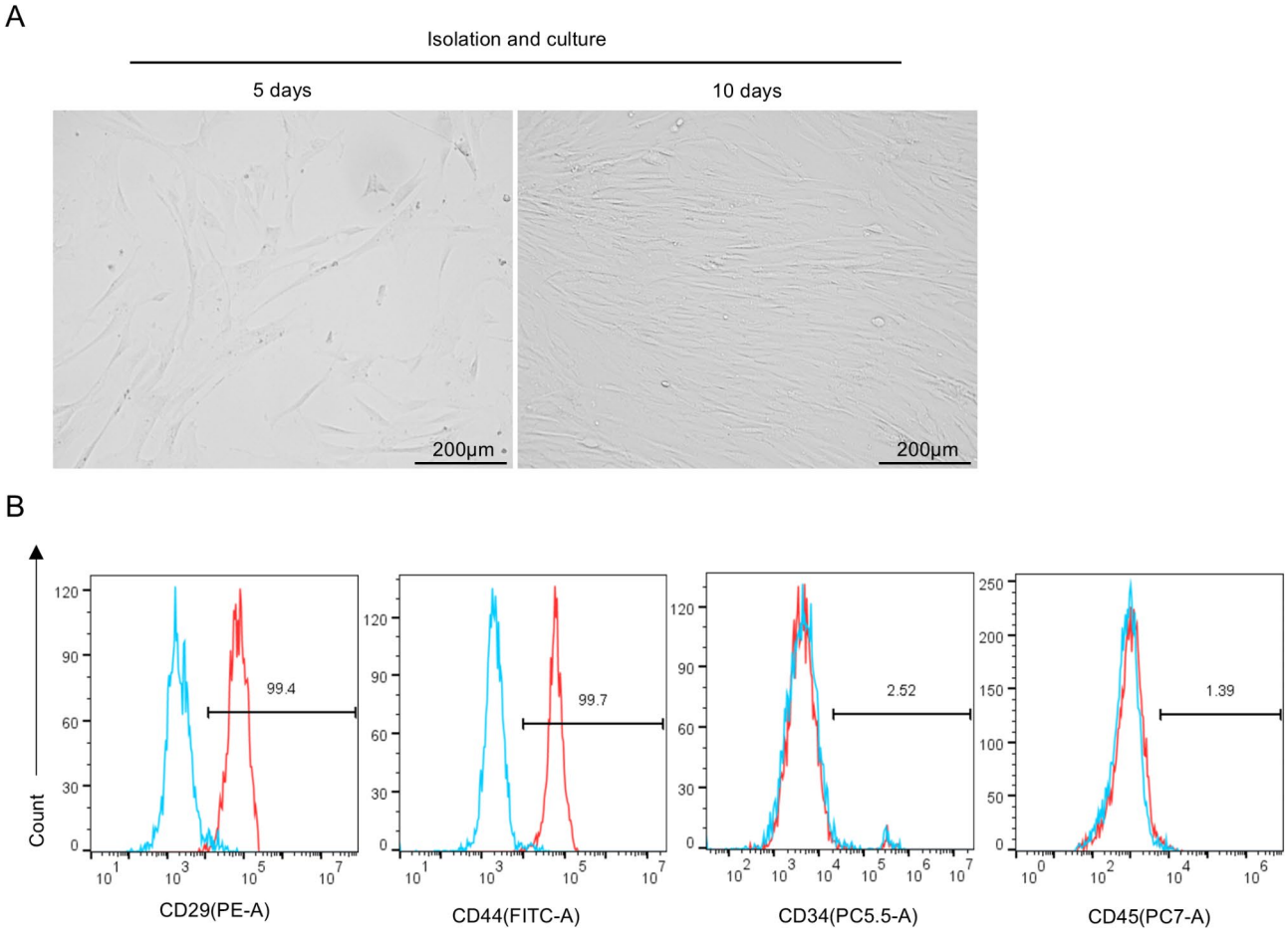

Fig. 1 Morphology and identification of rat BMSCs. (**A**) Microscopy images of BMSCs isolated and cultured for 5 days or 10 days. (**B**) Flow cytometry was used to identify the purity of the BMSCs using a fluorescently labelled antibody

and 8.75 ± 0.82%) (Fig. 2D-E). Data from western blotting showed that the level of anti-apoptotic protein Bcl-2 was lessened in response to DEX while protein levels of proapoptotic factors (Bax and cleaved caspase-3) were increased (Fig. 2F-I). The dysregulation of apoptotic markers was significantly reversed by three doses of icariin (Fig. 2F-I). The inhibitory effect of the medium dose of icarrin on cell apoptosis is comparable to that of PTH (Fig. 2D-I).

Icariin activates the PI3K-AKT-UTX/EZH2 signaling

Western blotting was performed to quantify protein levels of factors involved in the PI3K-AKT-UTX/EZH2 signaling in rat BMSCs. Figure 3A-B revealed that the phosphorylated levels of PI3K and AKT were markedly reduced by DEX ($^{***}p < 0.001$), and the alteration was rescued by icariin treatment ($^{\#\#\#}p < 0.001$). The finding suggests that icariin activates the PI3K/AKT signaling in the cell model of femoral head osteonecrosis. Moreover, UTX level was reduced while H3K27me3 level was increased in the DEX group ($^{***}p < 0.001$), and the changes were counteracted by icariin treatment ($^{\#\#\#}p < 0.001$) (Fig. 3A, C). The increase in EZH2 protein level induced by DEX was reversed by icariin. The alterations of phosphorylated EZH2 levels were in opposite to changes in EZH2 levels (Fig. 3A, C). Importantly, the influence of icariin on the PI3K-AKT-UTX/EZH2 signaling is comparable to that of PTH. In conclusion, icariin increased UTX level while reducing H3K27me3 and EZH2 levels via activation of the PI3K/AKT signaling.

Icariin promotes osteogenic differentiation of BMSCs by overexpressing UTX or silencing EZH2

Given that the medium dose of icariin most significantly improved cell viability and repressed cell apoptosis, icariin-M (1 μM) was selected for following experiments. Since icariin upregulated UTX and reduced EZH2 level, we overexpressed UTX and silenced EZH2 in rat BMSCs by transfecting the respective plasmids to explore whether UTX overexpression or EZH2 silencing exerts similar effects on osteogenic and adipogenic differentiation as observed with icariin treatment. Figure 4A-B showed that UTX expression was successfully amplified, while EZH2 level was markedly lessened post

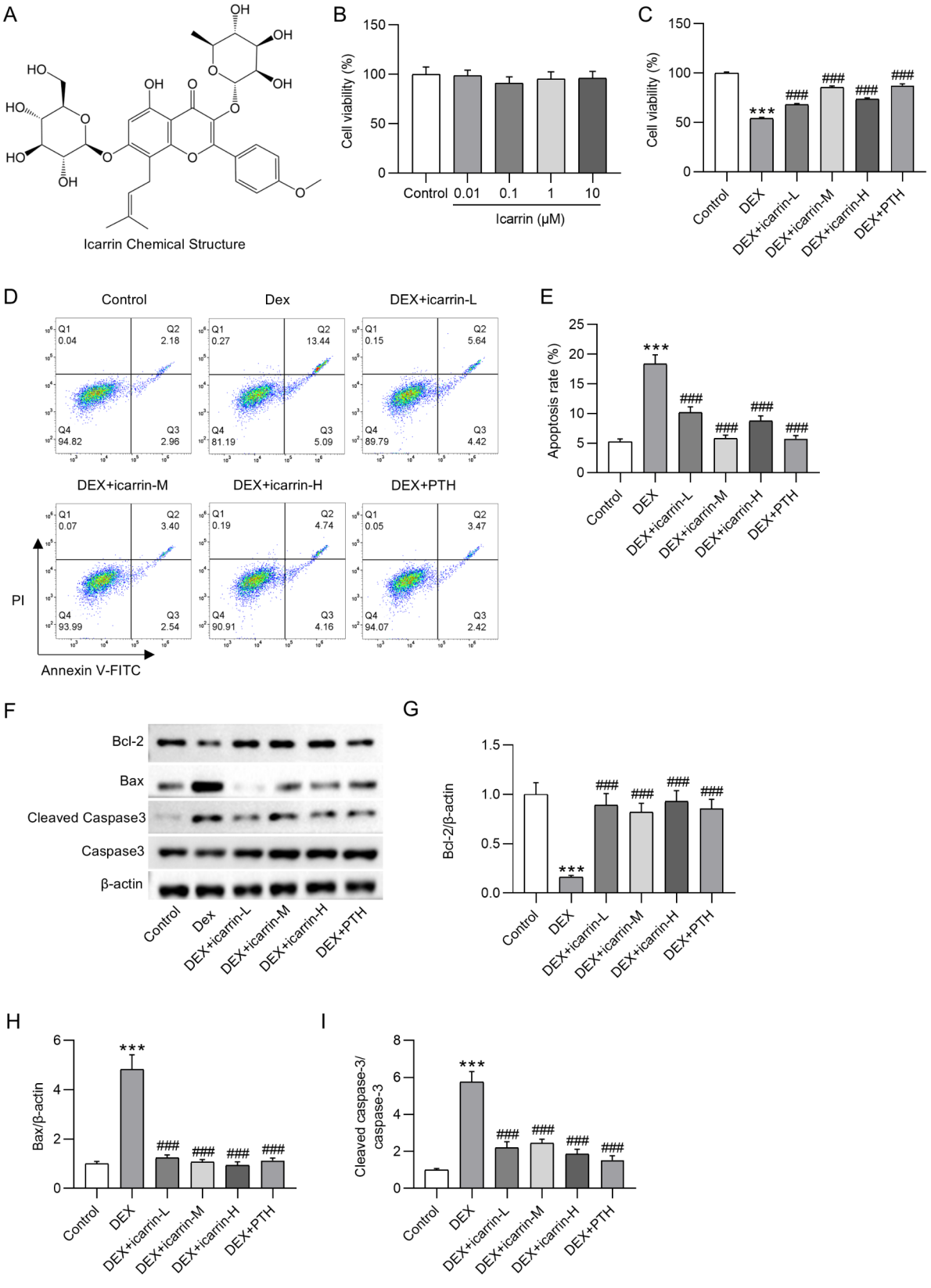

Fig. 2 (See legend on next page.)

(See figure on previous page.)

Fig. 2 Icariin attenuates dexamethasone (DEX)-induced apoptosis of rat BMSCs. (**A**) Chemical structure of icariin ($C_{33}H_{40}O_{15}$). (**B**) Cell counting kit-8 (CCK-8) was performed to determine the toxicity of various concentrations of icariin to rat BMSCs. (**C**-**E**) CCK-8 and flow cytometry analyses were performed to examine cell viability (**C**) and apoptosis (**D**-**E**) in control, DEX, DEX + icariin-L (low)/-M (medium)/-H (high), and DEX + parathyroid hormone (PTH) groups. (**F**-**I**) Protein levels of apoptotic markers in rat BMSCs of six groups were quantified by western blotting. $^{***}p < 0.001$ versus control group, $^{\#}p < 0.05$, $^{\#\#\#}p < 0.001$ versus DEX group

transfection. As displayed by images of Alizarin red S staining, there were less calcium nodules in the DEX group than the control group, while icariin, UTX overexpression, or EZH2 knockdown significantly improved the mineralization of rat BMSCs (Fig. 4C). The mRNA and protein levels of osteogenesis-related factors (Bmp2 and Runx2) were reduced in response to DEX treatment ($^{***}p < 0.001$), and the reduction was rescued by icariin, UTX overexpression, or EZH2 depletion (Fig. 4D-H). In summary, overexpressed UTX or silenced EZH2 exerted similar promoting effects on osteogenesis as icariin, indicating that icariin facilitated osteogenic differentiation of BMSCs through upregulation of UTX or downregulation of EZH2.

Like icariin, overexpressed UTX or silenced EZH2 exerts similar inhibitory effects on adipogenic differentiation of BMSCs

Oil red O staining was performed to assess the influence of icariin, UTX overexpression, or EZH2 knockdown on adipogenic differentiation. Compared with the control group, the DEX group showed abundant fat droplets (Fig. 5A). In the last four groups, the size and number of fat droplets were noticeably reduced in contrast to those in the DEX group (Fig. 5A). PPAR-γ and C/EBPα are factors related to adipogenic differentiation, which were highly expressed in DEX-stimulated BMSCs at mRNA and protein levels (Fig. 5B-F). The upregulation of PPAR-γ and C/EBPα levels induced by DEX was prominently lowered in the icariin-M, UTX, sh-EZH2, and positive control PTH groups (Fig. 5B-F). The findings suggest that icariin inhibits adipogenic differentiation of BMSCs in the context of DEX, and the similar inhibitory effects were achieved by UTX overexpression or EZH2 depletion.

Inhibition of the PI3K/Akt signaling counteracts the effects of icariin on UTX and EZH2 levels as well as osteogenic differentiation

An inhibitor for PI3K/Akt signaling (LY294002) was used for BMSC treatment to explore whether icariin promotes osteogenic differentiation via the PI3K/Akt signaling. Compared with UTX and EZH2 protein levels in the sole DEX group, icariin-induced UTX upregulation and EZH2 downregulation in DEX-stimulated BMSCs (Fig. 6A-B, $^{\#\#\#}p < 0.001$). While the changes in UTX and EZH2 protein levels mediated by icariin were counteracted by LY294002 in DEX-treated BMSCs (Fig. 6A-B, $^{\&\&\&}p < 0.001$). The results suggest that inhibition of the PI3K/Akt signaling abolished the regulatory effects of icariin on UTX and EZH2. Results from Alizarin red S showed that icariin rescued DEX-induced decrease in the number of calcium nodules. Moreover, the number of calcium nodules in the DEX + icariin-M + LY294002 group was significantly diminished compared with that in the DEX + icariin-M group and was close to the value in the DEX group (Fig. 6C-D). Furthermore, the reduction of Bmp2 and Runx2 at mRNA and protein levels in DEX-stimulated BMSCs ($^{***}p < 0.001$) was reversed by icariin treatment ($\#p < 0.05$, $\#\#p < 0.01$, $\#\#\#p < 0.001$), while the trend mediated by icariin was restored by LY294002 ($^{\&\&}p < 0.01$, $^{\&\&\&}p < 0.001$). The findings indicate that LY294002 countervailed the promoting impact of icariin on osteogenic differentiation in vitro.

Inhibition of the PI3K/Akt signaling reverses the inhibitory effect of icariin on adipogenic differentiation

Results from Oil-red O staining revealed that DEX-induced abundant fat droplets were ameliorated by icariin (Fig. 7A). While the inhibitory effect of icariin on the formation of fat droplets was reversed by LY294002 (Fig. 7A). In addition, DEX-induced high levels of PPAR-γ and C/EBPα were reduced in response to icariin treatment (Fig. 7B-F). However, the suppression of icariin on mRNA and protein levels of adipogenic differentiation-related factors was countervailed by LY294002 (Fig. 7B-F, $^{\&\&\&}p < 0.001$). The results suggest that inhibition of the PI3K/Akt signaling reverses the inhibitory effect of icariin on adipogenic differentiation.

Icariin exerts a protective role in the rat model of SONFH

The rat model of SONFH was established to investigate the in vivo role of icariin. The micro-CT analysis displayed that levels of trabeculae parameters including bone volume (BV), bone volume fraction (BV/TV), and number of trabeculae (Tb.N) were reduced in the SONFH model group compared with those in the control group (Fig. 8A-C, $^{**}p < 0.01$, $^{***}p < 0.001$). While the trabecular gap was enlarged in the SONFH group, as evidenced by the increase of trabecular separation (Tb.Sp) in model rats (0.68 ± 0.06 mm versus control 0.32 ± 0.03 mm) (Fig. 8D). The changes of trabeculae parameters in SONFH model rats were all counteracted by icariin administration (Fig. 8A-D, $^{\#}p < 0.05$, $^{\#\#}p < 0.01$, $^{\#\#\#}p < 0.001$). H&E staining revealed that the cartilage layer of the femoral head was thickened, and the bone

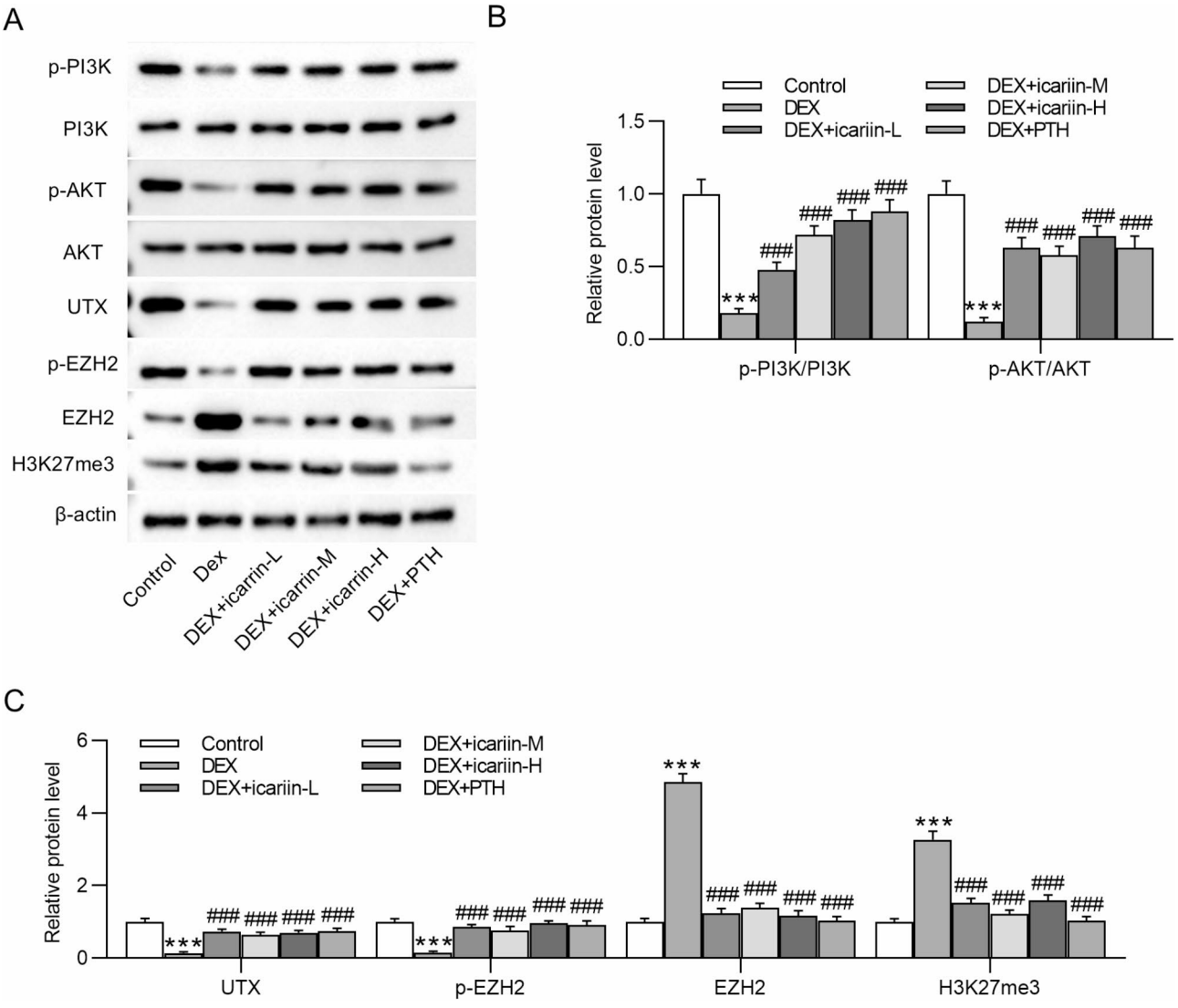

Fig. 3 Icariin activates the PI3K-AKT-UTX/EZH2 signaling in DEX-stimulated BMSCs. (**A**) Western blotting was performed to quantify protein levels of factors involved in the PI3K-AKT-UTX/EZH2 pathway. (**B**) The ratios of phosphorylated (p) PI3K/PI3K and p-AKT/AKT were measured in control, DEX, DEX + icariin-L/M/H, and DEX + PTH groups. (**C**) Quantification of UTX, EZH2, phosphorylated EZH2, and H3K27me3 levels in six groups. ***$p < 0.001$ versus control group, ###$p < 0.001$ versus DEX group

trabeculae displayed disorganized arrangement (Fig. 8E). Notably, the histopathological changes were ameliorated by icariin treatment (Fig. 8E). The activity of PI3K/Akt signaling was diminished in the femur tissues of SONFH group, and the alteration was rescued by the administration of icariin (Fig. 8F-G). UTX and p-EZH2 levels were diminished while EZH2 and H3K27me3 protein levels were elevated in rat femur tissues following SONFH modeling, and the changes were counteracted by icariin treatment (Fig. 8F&H). The results indicate that icariin ameliorates the damage of steroids to the structure of the femoral head and regulates the PI3K-AKT-UTX/EZH2 signaling in the rat model of SONFH.

A diagram showing how icariin promotes osteogenic differentiation of DEX-treated BMSCs via PI3K-AKT-UTX/EZH2 signaling

A diagram was used to clearly display the mechanism underlying the promotive effect of icariin on osteogenic differentiation. Figure 9 showed that icariin activates the PI3K/Akt signaling, and the activation of Akt led to UTX upregulation and EZH2 downregulation, resulting in the removement of H3K27me3 and eventually promoting osteogenic differentiation, keeping the balance of osteogenesis and adipogenesis, and preventing BMSC apoptosis. In conclusion, icariin promotes osteogenic differentiation of DEX-treated BMSCs and inhibits cell apoptosis by activating the PI3K-AKT-UTX/EZH2 signaling.

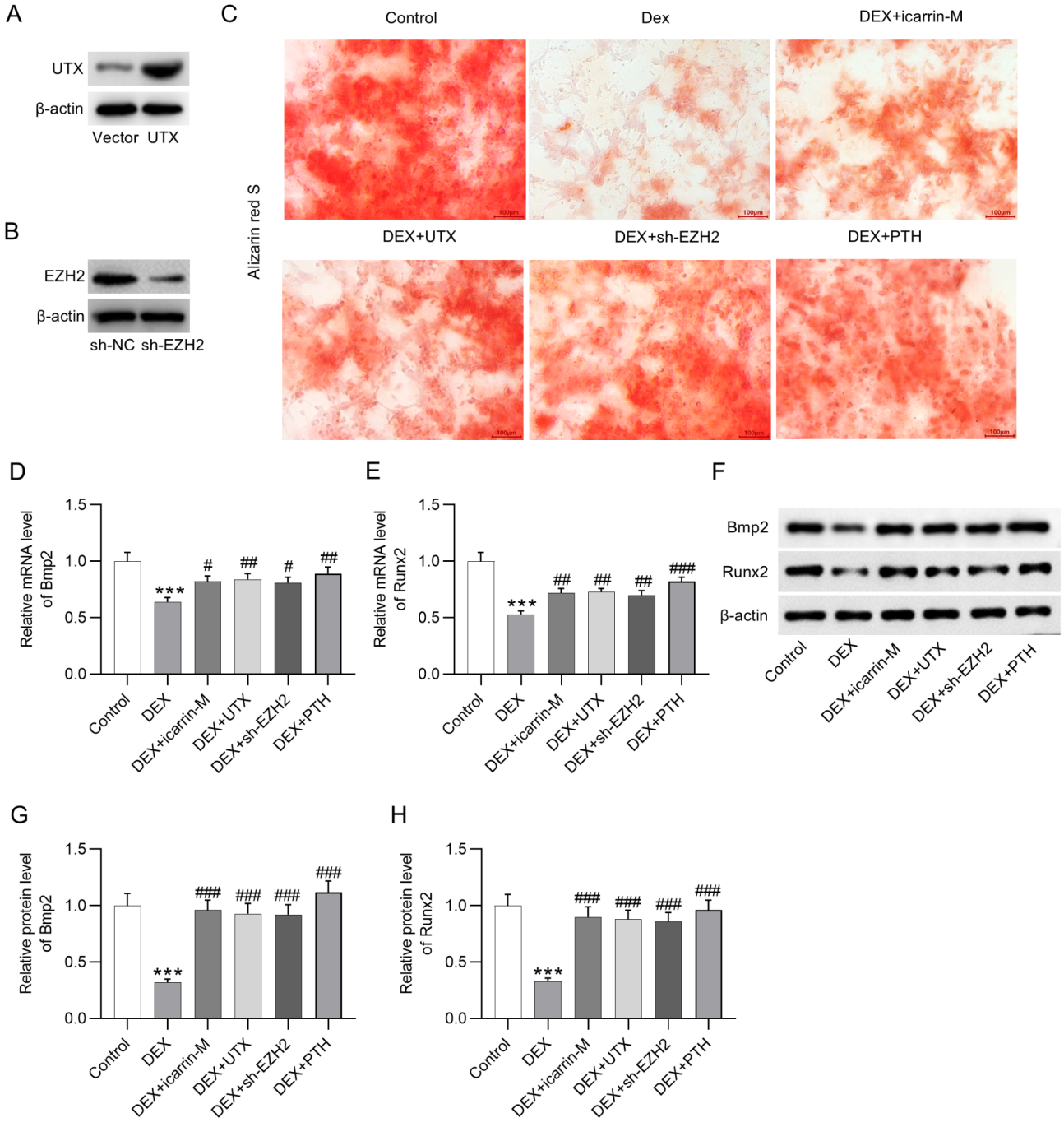

Fig. 4 Icariin promotes osteogenic differentiation of BMSCs by overexpressing UTX or silencing EZH2. (**A**-**B**) Western blot was performed to measure the efficacy of UTX overexpression (A) or the efficiency of EZH2 knockdown (B) post transfection of pORF-UTX or sh-EZH2 to rat BMSCs. (**C**) Alizarin red S staining was performed to evaluate osteogenic differentiation of BMSCs in response to DEX, icariin, PTH, UTZ overexpression, or EZH2 depletion. (**D**-**E**) RT-qPCR was conducted to measure mRNA levels of osteogenesis-related factors (Bmp2 and Runx2) in the control, DEX, DEX + icariin-M, DEX + UTX, DEX + sh-EZH2, and DEX + PTH groups. (**F**-**H**) Western blotting was performed to measure the effect of icariin, UTX overexpression, EZH2 deficiency, or PTH on protein levels of Bmp2 and Runx2. ***$p < 0.001$ versus control group, $^{\#}p < 0.05$, $^{\#\#}p < 0.01$, $^{\#\#\#}p < 0.001$ versus DEX group

Discussion

ONFH is frequently observed in skeletally immature patients. The treatment of ONFH remains a subject of debate, characterized by limited evidence and variable outcomes [5]. Stable research areas in the field of hip-preserving treatment for early ONFH encompass core decompression, osteotomy, bone transplantation, and cell therapy [3, 33]. However, some studies hold that core decompression is not as effective as other joint-preserving methods [34]. Migliorini F et al. has

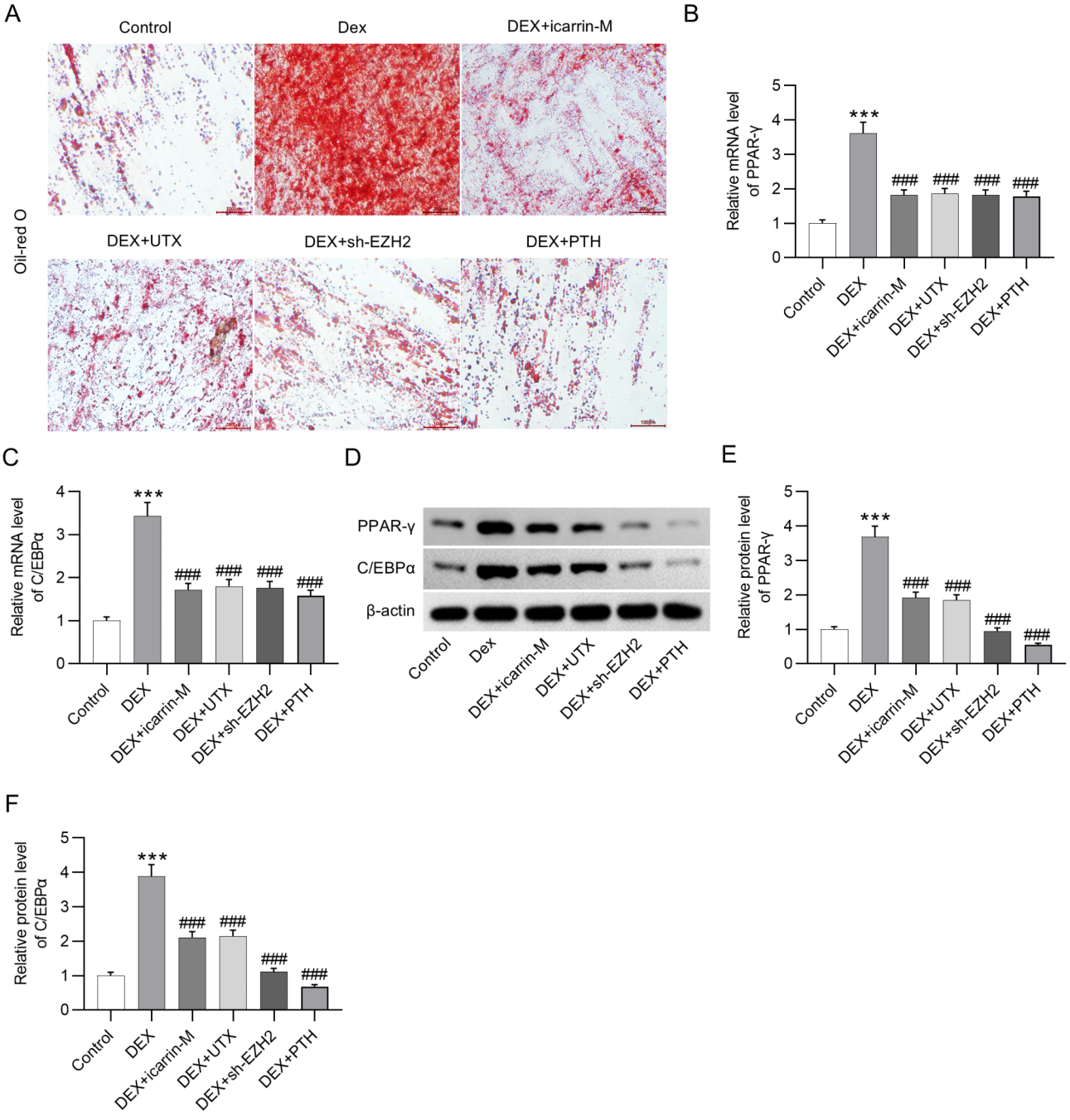

Fig. 5 Like icariin, overexpressed UTX or silenced EZH2 exerts the same inhibitory effect on adipogenic differentiation of BMSCs. (**A**) Oil-red O staining was performed to measure the influence of icariin, UTX upregulation, EZH2 depletion, or PTH on adipogenic differentiation of BMSCs in presence of DEX. (**B**-**C**) RT-qPCR was performed to assess mRNA levels of adipogenesis-related markers (PPAR-γ and C/EBPα) in the control, DEX, DEX + icariin-M, DEX + UTX, DEX + sh-EZH2, and DEX + PTH groups. (**D**-**F**) PPAR-γ and C/EBPα protein levels in BMSCs of abovementioned groups were measured by western blotting. ***$p < 0.001$ versus control group, ###$p < 0.001$ versus DEX group

demonstrated that the combination of core decompression and bone marrow-derived cell therapies alleviates pain and reduced the rate of total hip arthroplasty [35]. In the long term, it is imperative to determine more effective therapeutic strategy for managing ONFH.

Evidence shows that BMSC apoptosis and abnormal differentiation, disorder of lipid metabolism and coagulation pathway, unbalance of osteoclasts and osteoblasts, and poor vascularization repair are all possible pathogenic factors for SONFH [36, 37]. DEX-treated BMSCs are frequently used as cell models for investigation of

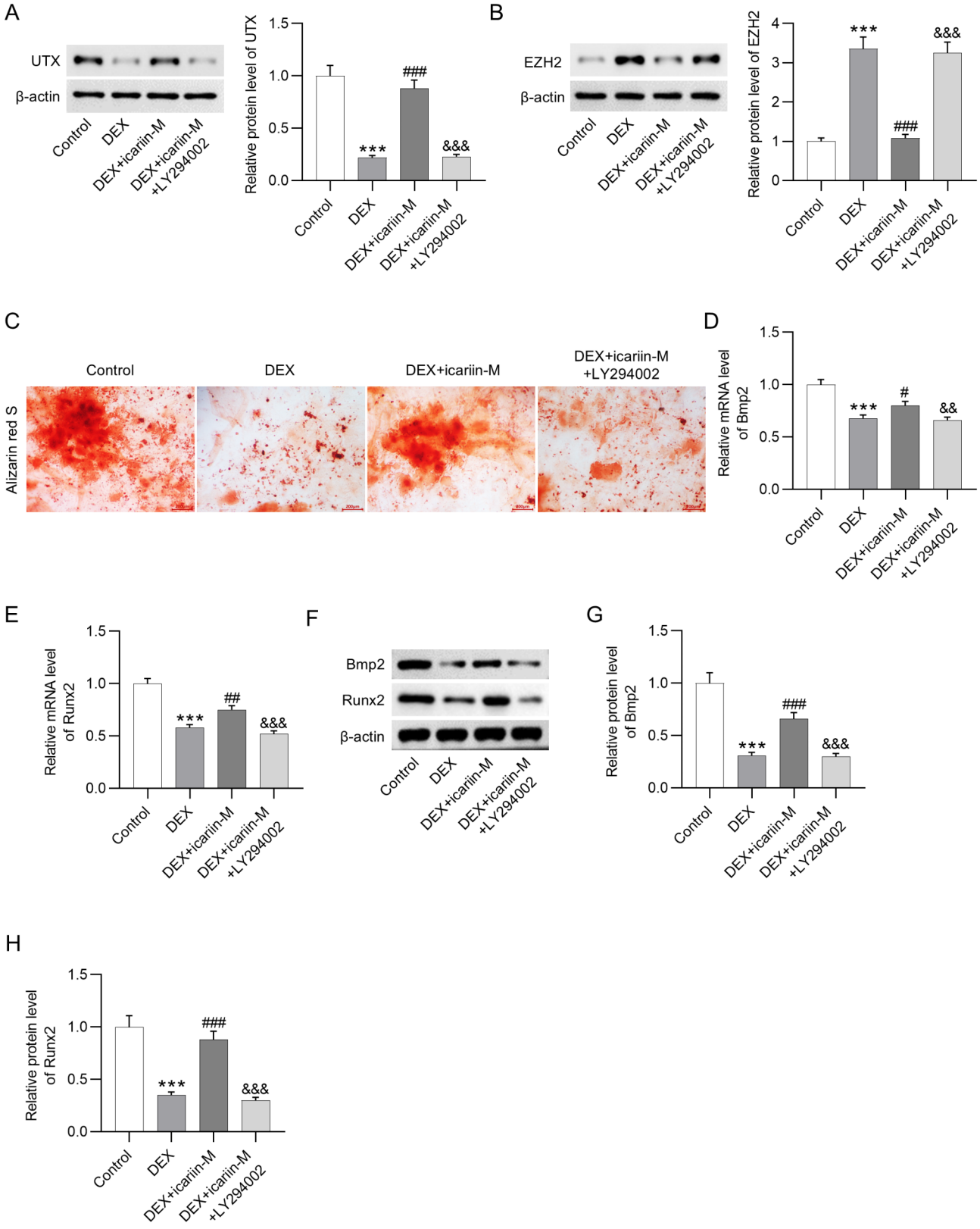

Fig. 6 Inhibition of the PI3K/Akt signaling counteracts the effects of icariin on UTX and EZH2 levels as well as osteogenic differentiation. **A-B**. Western blotting was performed to measure UTX and EZH2 protein levels in BMSCs of control, DEX, DEX + icariin-M, and DEX + icariin-M + LY294002 groups. **C**. Alizarin red S staining was performed to evaluate osteogenic differentiation of BMSCs in each group. **D-E**. RT-qPCR was conducted to measure mRNA levels of osteogenesis-related factors (Bmp2 and Runx2) in each group. **F-H**. Protein levels of Bmp2 and Runx2 in BMSCs were quantitated by western blotting. $^{***}p < 0.001$ versus control group. $^{\#}p < 0.05$, $^{\#\#}p < 0.01$, $^{\#\#\#}p < 0.001$ versus DEX group. $^{\&\&}p < 0.01$, $^{\&\&\&}p < 0.001$ versus DEX + icariin-M group

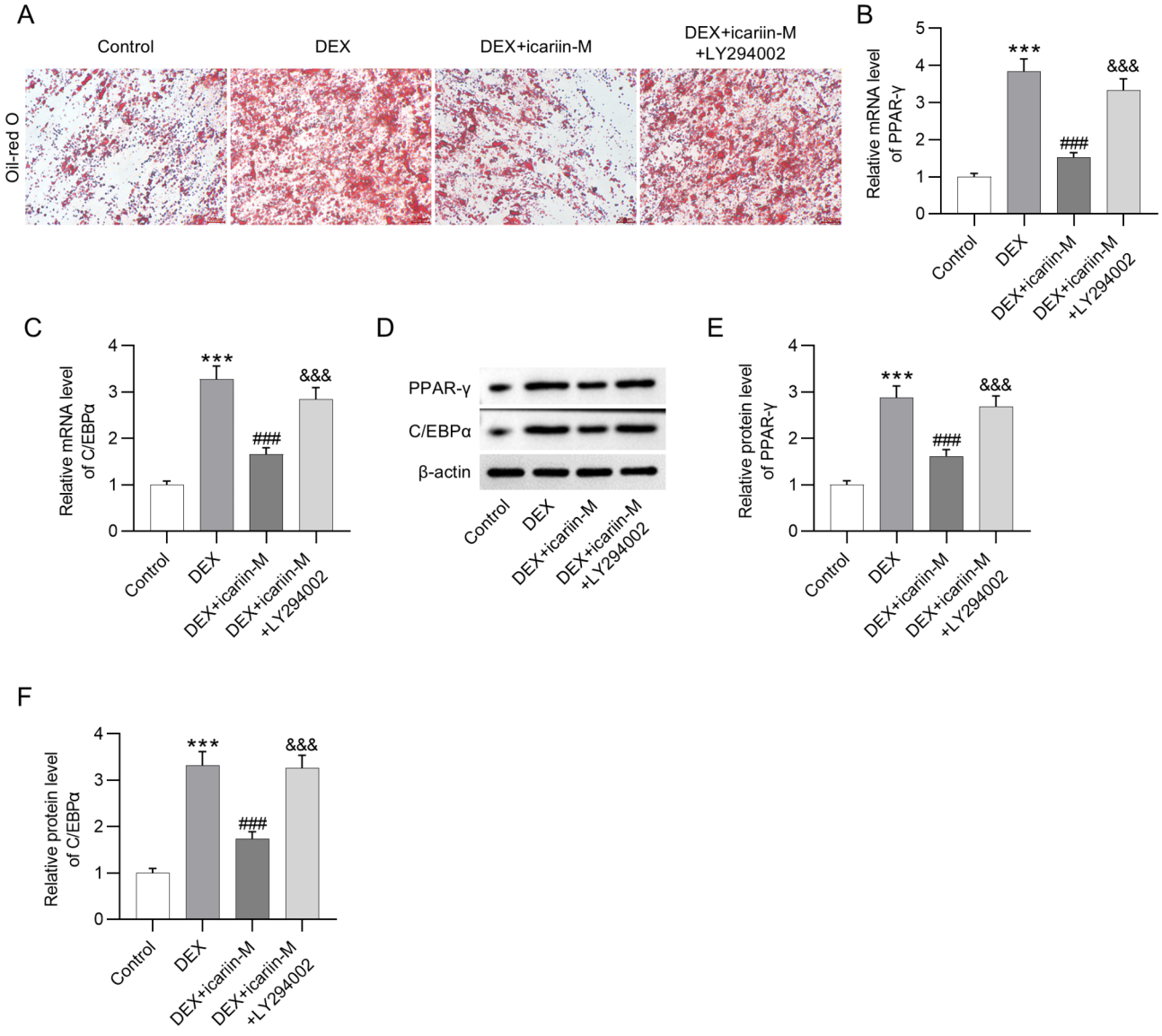

Fig. 7 Inhibition of the PI3K/Akt signaling reverses the inhibitory effect of icariin on adipogenic differentiation. **A**. Oil-red O staining was performed to measure adipogenic differentiation of BMSCs in control, DEX, DEX + icariin-M, and DEX + icariin-M + LY294002 groups. **B-C**. RT-qPCR was performed to assess mRNA levels of adipogenesis-related markers (PPAR-γ and C/EBPα) in BMSCs of each group. **D-F**. Western blotting was performed to measure protein levels of PPAR-γ and C/EBPα in BMSCs of each group. $^{***}p < 0.001$ versus control group. $^{###}p < 0.001$ versus DEX group. $^{&&&}p < 0.001$ versus DEX + icariin-M group

SONFH [15, 16]. Consistent with previous studies, DEX treatment reduced BMSC viability and repressed osteogenic differentiation while promoting cell apoptosis and adipogenic differentiation. This study not only demonstrated that icariin counteracted these changes mediated by DEX but also highlighted the axis of PI3K/AKT-UTX/EZH2 regulated by icariin. Moreover, a recent study has shown that epidermal growth factor (EGF) signaling can regulate bone homeostasis by regulating osteoblast differentiation and by stimulating the proliferation of osteoblasts and osteoclasts [38]. Previously, it was reported that icariin activates the EGF/EGF receptor pathway in porcine aorta endothelial cells [39]. Therefore, future studies could investigate the impact of icariin on the EGF signaling in osteoblast differentiation.

Our viewpoint of activating PI3K/AKT signaling to increase the viability and osteogenic differentiation of BMSCs is consistent with a published article. Xin et al. verified that circ_0066523 facilitates BMSC proliferation and differentiation by activating AKT signaling via epigenetically repression of PTEN [40]. However, contrary findings were reported in another study. As described by Ma et al., extracellular vesicles from BMSCs protect glucocorticoid-induced bone microvascular endothelial cells

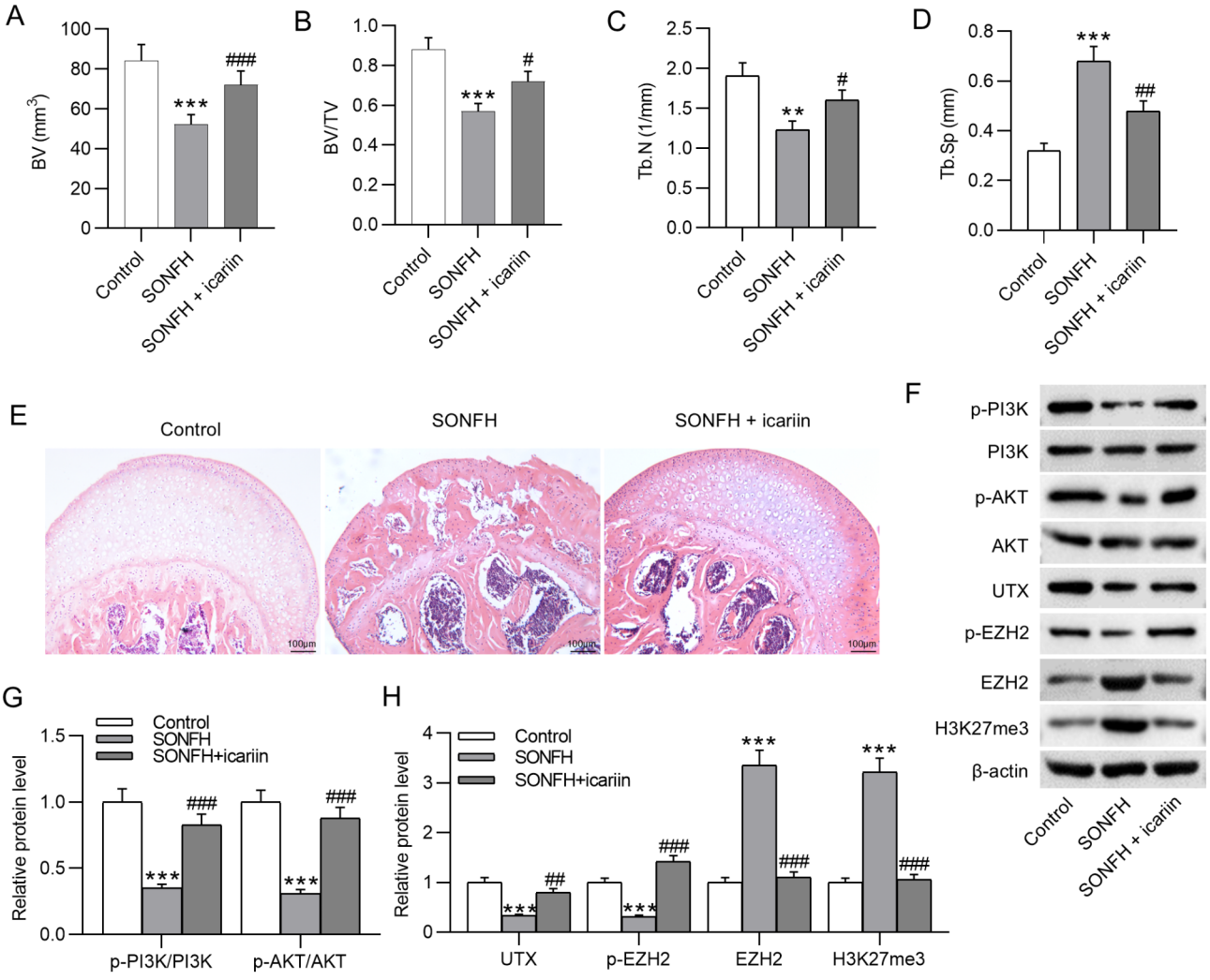

Fig. 8 Icariin exerts a protective role in the rat model of SONFH. **A-D**. After the modeling of SONFH in rats, micro-computed tomography (micro-CT) analysis was used to measure trabecular parameters including bone volume (BV), bone volume fraction (BV/TV), trabecular number (Tb.N), and trabecular separation (Tb.Sp) in rat femoral samples of control, SONFH, and SONFH + icariin groups. **E**. Hematoxylin-Eosin (H&E) staining was conducted to evaluate histopathological changes in femoral samples. **F-H**. Western blotting was performed to measure protein levels of factors involved in the PI3K-AKT-UTX/EZH2 signaling in femoral samples. $^{**}p < 0.01$, $^{***}p < 0.001$ versus control group. $^{\#}p < 0.05$, $^{\#\#}p < 0.01$, $^{\#\#\#}p < 0.001$ versus SONFH group

from injury by inhibiting the PI3K/AKT/mTOR signaling to activate autophagy [41]. The difference may be due to various cell types and the pleiotropic impacts of the PI3K signaling.

H3K27me3, a prominent epigenetic mark associated with gene silencing, is recognized as one of the most prevalent epigenetic signatures [42]. H3K27me3 depletion can lead to a decrease in the specification of mesenchymal stem cells (MSCs) into adipocytes and has also been discovered to coordinate osteoblast activity and bone formation in mice [43, 44]. In this study, icariin induced H3K27me3 depletion in BMSCs by upregulating UTX and downregulating EZH2 via PI3K/AKT. UTX can maintain its occupancy at the promoters of Runx2 and osterix, thereby sustaining osteogenic gene transcription [45]. Moreover, UTX reduces H3K27me3 enrichment in the Dkk1 promoter [45]. EZH2 is a H3K27 methyltransferase and is required for bone formation [46]. EZH2 can enhance the modification of H3K27me3 on the promoter of Foxo1 and thus activate genes involved in antioxidant defense in BMSCs [47]. These articles may explain the depletion of H3K27me3 induced by UTX overexpression and EZH2 knockdown in this study. EZH2 was found to promote adipogenesis by disrupting Wnt/β-catenin signaling in mouse peripheral preadipocytes [48]. Consistently, the adipogenic differentiation of BMSCs mediated by DEX was repressed by EZH2 depletion in the current work.

In conclusion, the study first explains that icariin prevents BMSCs from DEX-induced cell apoptosis and abnormal osteogenic and adipogenic differentiation by activating the PI3K/AKT signaling to upregulate UTX

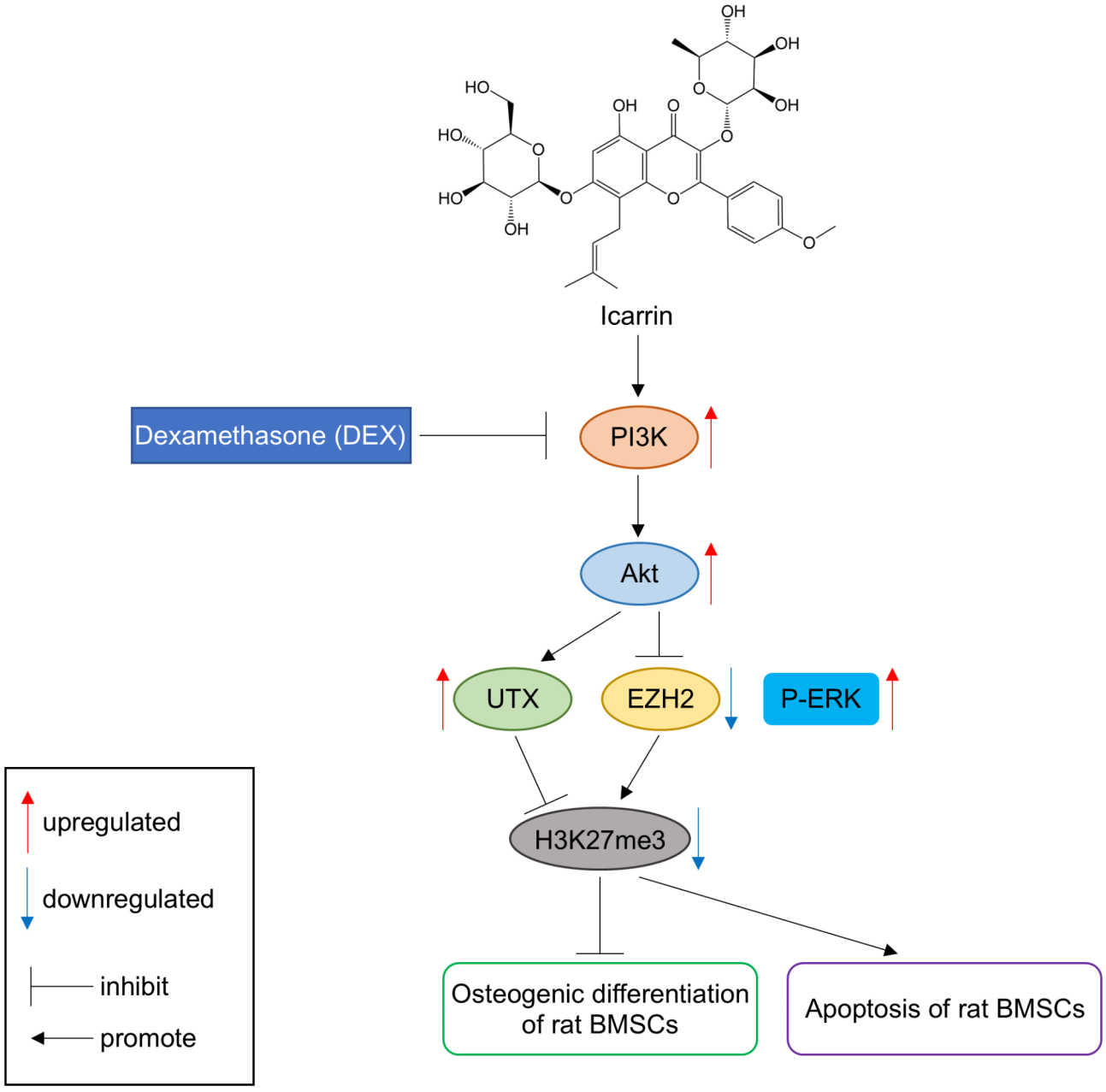

Fig. 9 A diagram showing how icariin promotes osteogenic differentiation of DEX-treated BMSCs via PI3K-AKT-UTX/EZH2 signaling

and silence EZH2, finally inducing H3K27me3 depletion to alter the expression of osteogenesis-related factors. The limitation of the study is that the animal model of SONFH was not established for further verification. For future work, targeting the icariin/PI3K-AKT-UTX/EZH2 pathway may have therapeutical potential for the treatment of SONFH. In addition, the extensive expertise accumulated in the culture and characterization of bone marrow-derived human mesenchymal stem cells has predictably resulted in a diverse array of clinical trial applications [49, 50]. Therefore, further in-depth studies are still required to fully explore the potential of BMSCs in treating SONFH.

Supplementary Information

The online version contains supplementary material available at https://doi.org/10.1186/s13018-025-05697-0.

Supplementary Material 1

Supplementary Material 2

Supplementary Material 3

Acknowledgements
Not applicable.

Author contributions
Wei Ji and Guoqing Gong conceived and designed the experiments. Wei Ji, Guoqing Gong, Yuanhang Liu, Yan Liu, Jie Zhang and Qiang Li carried out the experiments. Wei Ji, Guoqing Gong, Yuanhang Liu, Yan Liu, Jie Zhang and Qiang Li analyzed the data. Wei Ji, Guoqing Gong and Qiang Li drafted the manuscript. All authors agreed to be accountable for all aspects of the work. All authors have read and approved the final manuscript.

Funding
This work is supported by Wuhan Traditional Chinese Medicine Research Project (Approval number: WZ22Q14).

Data availability
The datasets used or analyzed during the current study are available from the corresponding author on reasonable request.

Declarations

Ethical approval
This study received approval from the Animal Ethics Committee of Wuhan Myhalic Biotechnology Co., Ltd (approval number: HLK-202309296; approval date: September 21, 2023).

Competing interests
The authors declare no competing interests.

Author details
[1]Department of Plastic Surgery, Tongren Hospital of Wuhan University (Wuhan Third Hospital), Wuhan 430060, China
[2]Department of Otolaryngology, Wuhan Third Hospital (Tongren Hospital of Wuhan University), Wuhan 430060, China
[3]Department of Foot and Ankle, Nanchang Hongdu Hospital of Traditional Chinese Medicine, No.264 Minde Road, Donghu District, Nanchang 330000, China

Received: 21 October 2024 / Accepted: 8 March 2025
Published online: 18 March 2025

References

1. Chen XJ, Shen YS, He MC, Yang F, Yang P, Pang FX, He W, Cao YM, Wei QS. Polydatin promotes the osteogenic differentiation of human bone mesenchymal stem cells by activating the BMP2-Wnt/β-catenin signaling pathway. Biomed Pharmacother. 2019;112:108746.
2. Yang F, Zhang X, Song T, Li X, Lv H, Li T, Zhao J, Liu Z, Zhang X, Hou Y, et al. Huogu injection alleviates SONFH by regulating adipogenic differentiation of BMSCs via targeting the miR-34c-5p/MDM4 pathway. Gene. 2022;838:146705.
3. Quaranta M, Miranda L, Oliva F, Aletto C, Maffulli N. Osteotomies for avascular necrosis of the femoral head. Br Med Bull. 2021;137(1):98–111.
4. Zhao D, Zhang F, Wang B, Liu B, Li L, Kim SY, Goodman SB, Hernigou P, Cui Q, Lineaweaver WC, et al. Guidelines for clinical diagnosis and treatment of osteonecrosis of the femoral head in adults (2019 version). J Orthop Translat. 2020;21:100–10.
5. Migliorini F, La Padula G, Oliva F, Torsiello E, Hildebrand F, Maffulli N. Operative management of avascular necrosis of the femoral head in skeletally immature patients: a systematic review. Life (Basel). 2022;12(2).
6. Migliorini F, Maffulli N, Baroncini A, Eschweiler J, Tingart M, Betsch M. Prognostic factors in the management of osteonecrosis of the femoral head: a systematic review. Surgeon. 2023;21(2):85–98.
7. Chai JL, Lu BW, Du HT, Wen MT, Liang XZ, Wang P. Pyroptosis -related potential diagnostic biomarkers in steroid-induced osteonecrosis of the femoral head. BMC Musculoskelet Disord. 2023;24(1):609.
8. Li W, Li W, Zhang W, Wang H, Yu L, Yang P, Qin Y, Gan M, Yang X, Huang L, et al. Exogenous melatonin ameliorates steroid-induced osteonecrosis of the femoral head by modulating ferroptosis through GDF15-mediated signaling. Stem Cell Res Ther. 2023;14(1):171.
9. Zheng C, Wu Y, Xu J, Liu Y, Ma J. Exosomes from bone marrow mesenchymal stem cells ameliorate glucocorticoid-induced osteonecrosis of femoral head by transferring microRNA-210 into bone microvascular endothelial cells. J Orthop Surg Res. 2023;18(1):939.
10. Zhang F, Yan Y, Peng W, Wang L, Wang T, Xie Z, Luo H, Zhang J, Dong W. PARK7 promotes repair in early steroid-induced osteonecrosis of the femoral head by enhancing resistance to stress-induced apoptosis in bone marrow mesenchymal stem cells via regulation of the Nrf2 signaling pathway. Cell Death Dis. 2021;12(10):940.
11. Wang J, Wang T, Zhang F, Zhang Y, Guo Y, Jiang X, Yang B. Roles of circular RNAs in osteogenic differentiation of bone marrow mesenchymal stem cells (Review). Mol Med Rep. 2022;26(1).
12. Hu Y, Zhang Y, Ni CY, Chen CY, Rao SS, Yin H, Huang J, Tan YJ, Wang ZX, Cao J, et al. Human umbilical cord mesenchymal stromal cells-derived extracellular vesicles exert potent bone protective effects by CLEC11A-mediated regulation of bone metabolism. Theranostics. 2020;10(5):2293–308.
13. Giai Via A, McCarthy MB, de Girolamo L, Ragni E, Oliva F, Maffulli N. Making them commit: strategies to influence phenotypic differentiation in mesenchymal stem cells. Sports Med Arthrosc Rev. 2018;26(2):64–9.
14. Fang S, He T, You M, Zhu H, Chen P. Glucocorticoids promote steroid-induced osteonecrosis of the femoral head by down-regulating serum alpha-2-macroglobulin to induce oxidative stress and facilitate SIRT2-mediated BMP2 deacetylation. Free Radic Biol Med. 2024;213:208–21.
15. Sun Y, Liang M, Xing Y, Duan Y, Zhang S, Deng B, Xiang X, Zhou B. Cyasterone has a protective effect on steroid-induced osteonecrosis of the femoral head. PLoS ONE. 2023;18(10):e0293530.
16. Jia B, Jiang Y, Yao Y, Xu Y, Wang Y, Li T. Baicalin attenuates dexamethasone-induced apoptosis of bone marrow mesenchymal stem cells by activating the Hedgehog signaling pathway. Chin Med J (Engl). 2023;136(15):1839–47.
17. Song IH, Caplan AI, Dennis JE. Dexamethasone inhibition of confluence-induced apoptosis in human mesenchymal stem cells. J Orthop Res. 2009;27(2):216–21.
18. Chen Q, Liu Y, Ding X, Li Q, Qiu F, Wang M, Shen Z, Zheng H, Fu G. Bone marrow mesenchymal stem cell-secreted exosomes carrying microRNA-125b protect against myocardial ischemia reperfusion injury via targeting SIRT7. Mol Cell Biochem. 2020;465(1–2):103–14.
19. Li Y, Wang X. Chrysin attenuates high glucose-induced BMSC dysfunction via the activation of the PI3K/AKT/Nrf2 signaling pathway. Drug Des Devel Ther. 2022;16:165–82.
20. Chen H, Huang Y, Huang D, Wu Z, Li Y, Zhou C, Wei G. Protective effect of gigantol against hydrogen peroxide–induced apoptosis in rat bone marrow mesenchymal stem cells through the PI3K/Akt pathway. Mol Med Rep. 2018;17(2):3267–73.
21. Yao X, Jing X, Guo J, Sun K, Deng Y, Zhang Y, Guo F, Ye Y. Icariin protects bone marrow mesenchymal stem cells against Iron overload induced dysfunction through mitochondrial fusion and fission, PI3K/AKT/mTOR and MAPK pathways. Front Pharmacol. 2019;10:163.
22. Huang Z, Cheng C, Cao B, Wang J, Wei H, Liu X, Han Y, Yang S, Wang X. Icariin protects against glucocorticoid-induced osteonecrosis of the femoral head in rats. Cell Physiol Biochemistry: Int J Experimental Cell Physiol Biochem Pharmacol. 2018;47(2):694–706.
23. Cha TL, Zhou BP, Xia W, Wu Y, Yang CC, Chen CT, Ping B, Otte AP, Hung MC. Akt-mediated phosphorylation of EZH2 suppresses methylation of lysine 27 in histone H3. Science. 2005;310(5746):306–10.
24. Xia Y, Ikedo A, Lee JW, Iimura T, Inoue K, Imai Y. Histone H3K27 demethylase, Utx, regulates osteoblast-to-osteocyte differentiation. Biochem Biophys Res Commun. 2022;590:132–38.
25. Zhang XY, Li HN, Chen F, Chen YP, Chai Y, Liao JZ, Gan B, Chen DP, Li S, Liu YQ. Icariin regulates miR-23a-3p-mediated osteogenic differentiation of BMSCs via BMP-2/Smad5/Runx2 and WNT/β-catenin pathways in osteonecrosis of the femoral head. Saudi Pharm J. 2021;29(12):1405–15.
26. Meng CY, Xue F, Zhao ZQ, Hao T, Guo SB, Feng W. Influence of MicroRNA-141 on inhibition of the proliferation of bone marrow mesenchymal stem cells in steroid-induced osteonecrosis via SOX11. Orthop Surg. 2020;12(1):277–85.
27. Chen Y, Chen Y, Zhang S, Du X, Bai B. Parathyroid hormone-induced bone marrow mesenchymal stem cell chondrogenic differentiation and its repair of articular cartilage injury in rabbits. Med Sci Monit Basic Res. 2016;22:132–45.
28. Zhang H, Ding Y, Hou Y, Liu Y, Zhou Z, Nie H. Bone marrow mesenchymal stem cells derived miRNA-130b enhances epithelial sodium channel by targeting PTEN. Respir Res. 2020;21(1):329.
29. Zhou C, Hu G, Li Y, Zheng S. Polydatin accelerates osteoporotic bone repair by inducing the osteogenesis-angiogenesis coupling of bone marrow

mesenchymal stem cells via the PI3K/AKT/GSK-3β/β-catenin pathway. Int J Surg. 2024;111(1):411–25.
30. Li H, Zhang Y, Hao Y, Xu P, Wang X, Zhu B, Lu C, Xu K. Proanthocyanidins inhibit osteoblast apoptosis via the PI3K/AKT/Bcl-xL pathway in the treatment of steroid-induced osteonecrosis of the femoral head in rats. Nutrients. 2023;15(8).
31. Fang L, Zhang G, Wu Y, Li H, Li Z, Yu B, Wang B, Zhou L. Fibroblast growth factor 23 inhibition attenuates steroid-induced osteonecrosis of the femoral head through pyroptosis. Sci Rep. 2024;14(1):16270.
32. Qian Z, Zhu L, Li Y, Li Y, Wu Y, Fu S, Yang D. Icarrin prevents cardiomyocyte apoptosis in spontaneously hypertensive rats by inhibiting endoplasmic reticulum stress pathways. J Pharm Pharmacol. 2021;73(8):1023–32.
33. Wu T, Jiang Y, Tian H, Shi W, Wang Y, Li T. Systematic analysis of hip-preserving treatment for early osteonecrosis of the femoral head from the perspective of bibliometrics (2010–2023). J Orthop Surg Res. 2023;18(1):959.
34. Sadile F, Bernasconi A, Russo S, Maffulli N. Core decompression versus other joint preserving treatments for osteonecrosis of the femoral head: a meta-analysis. Br Med Bull. 2016;118(1):33–49.
35. Migliorini F, Maffulli N, Eschweiler J, Tingart M, Baroncini A. Core decompression isolated or combined with bone marrow-derived cell therapies for femoral head osteonecrosis. Expert Opin Biol Ther. 2021;21(3):423–30.
36. Huang C, Qing L, Xiao Y, Tang J, Wu P. Insight into steroid-induced ONFH: the molecular mechanism and function of epigenetic modification in mesenchymal stem cells. Biomolecules. 2023;14(1).
37. Chen K, Liu Y, He J, Pavlos N, Wang C, Kenny J, Yuan J, Zhang Q, Xu J, He W. Steroid-induced osteonecrosis of the femoral head reveals enhanced reactive oxygen species and hyperactive osteoclasts. Int J Biol Sci. 2020;16(11):1888–900.
38. Mangiavini L, Peretti GM, Canciani B, Maffulli N. Epidermal growth factor signalling pathway in endochondral ossification: an evidence-based narrative review. Ann Med. 2022;54(1):37–50.
39. Liu T, Qin XC, Li WR, Zhou F, Li GY, Xin H, Gong YQ, Xin ZC. Effects of icariin and icariside II on eNOS expression and NOS activity in porcine aorta endothelial cells. Beijing Da Xue Xue Bao Yi Xue Ban. 2011;43(4):500–4.
40. Xin W, Yuan S, Wang B, Qian Q, Chen Y. Hsa_circ_0066523 promotes the proliferation and osteogenic differentiation of bone mesenchymal stem cells by repressing PTEN. Bone Joint Res. 2021;10(8):526–35.
41. Ma J, Shen M, Yue D, Wang W, Gao F, Wang B. Extracellular vesicles from BMSCs prevent glucocorticoid-induced BMECs injury by regulating autophagy via the PI3K/Akt/mTOR pathway. Cells. 2022;11(13).
42. Crea F, Sun L, Mai A, Chiang YT, Farrar WL, Danesi R, Helgason CD. The emerging role of histone lysine demethylases in prostate cancer. Mol Cancer. 2012;11:52.
43. Jing H, Liao L, An Y, Su X, Liu S, Shuai Y, Zhang X, Jin Y. Suppression of EZH2 prevents the shift of osteoporotic MSC fate to adipocyte and enhances bone formation during osteoporosis. Mol Ther. 2016;24(2):217–29.
44. Sun Y, Cai M, Zhong J, Yang L, Xiao J, Jin F, Xue H, Liu X, Liu H, Zhang Y, et al. The long noncoding RNA lnc-ob1 facilitates bone formation by upregulating Osterix in osteoblasts. Nat Metab. 2019;1(4):485–96.
45. Wang FS, Lian WS, Lee MS, Weng WT, Huang YH, Chen YS, Sun YC, Wu SL, Chuang PC, Ko JY. Histone demethylase UTX counteracts glucocorticoid deregulation of osteogenesis by modulating histone-dependent and -independent pathways. J Mol Med. 2017;95(5):499–512.
46. Schwarz D, Varum S, Zemke M, Schöler A, Baggiolini A, Draganova K, Koseki H, Schübeler D, Sommer L. Ezh2 is required for neural crest-derived cartilage and bone formation. Development. 2014;141(4):867–77.
47. Su X, Zhang H, Lei F, Wang R, Lin T, Liao L. Epigenetic therapy attenuates oxidative stress in BMSCs during ageing. J Cell Mol Med. 2022;26(2):375–84.
48. Wang L, Jin Q, Lee JE, Su IH, Ge K, Histone. H3K27 methyltransferase Ezh2 represses Wnt genes to facilitate adipogenesis. Proc Natl Acad Sci U S A. 2010;107(16):7317–22.
49. Kay AG, Dale TP, Akram KM, Mohan P, Hampson K, Maffulli N, Spiteri MA, El Haj AJ, Forsyth NR. BMP2 repression and optimized culture conditions promote human bone marrow-derived mesenchymal stem cell isolation. Regen Med. 2015;10(2):109–25.
50. Barnaba S, Papalia R, Ruzzini L, Sgambato A, Maffulli N, Denaro V. Effect of pulsed electromagnetic fields on human osteoblast cultures. Physiother Res Int. 2013;18(2):109–14.

Publisher's note